The recognition of tumors …

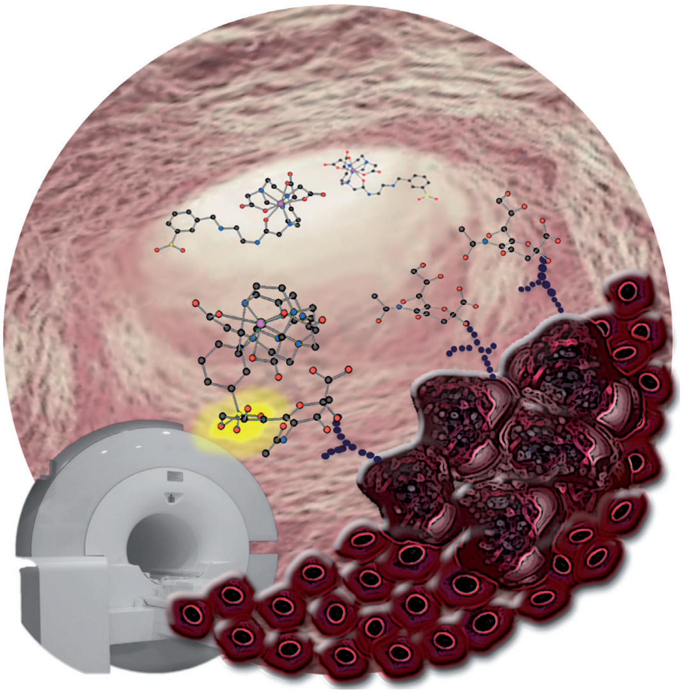

… is possible through the dynamic formation of cyclic boronate esters between the diol moiety of the overexpressed marker sialic acid and a phenylboronic acid (pba) targeting vector. In their Communication on page 1161 ff., K. Djanashvili et al. demonstrate an MRI signal intensity enhancement at the tumor site as a result of the accumulation and prolonged retention of a Gd^{III}-dota-en-pba targeting contrast agent after its intravenous injection into a melanoma mouse xenograft.

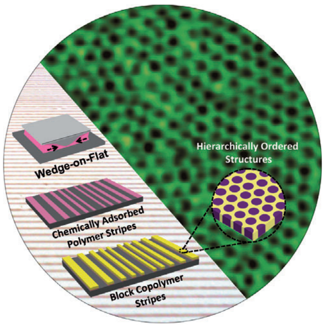

Self-Assembly

The formation of hierarchically ordered structures composed of diblock copolymers through two consecutive self-assembly processes is presented by Lin et al. in their Communication on page 1122 ff.

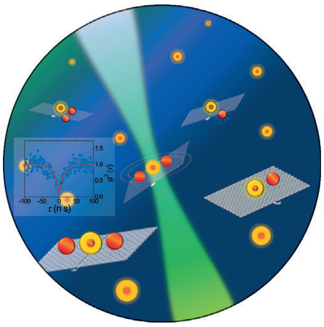

Quantum Dots

In their Communication on page 1193 ff., J. A. Liddle et al. describe a strategy to manipulate quantum-dot lifetimes using nearby gold nanoparticles on DNA origami templates.

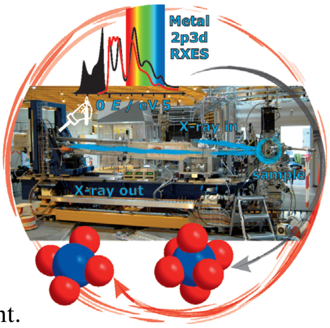

X-ray Spectroscopy

For cobalt(II) carboxylates, M. M. van Schooneveld, F. M. F. de Groot et al. show in their Communication on page 1170 ff. that 2p3d resonant X-ray emission spectroscopy allows the determination of the metal-ion coordination environment.

How to contact us:

Editorial Office:
E-mail: angewandte@wiley-vch.de
Fax: (+49) 6201–606-331
Telephone: (+49) 6201–606-315

Reprints, E-Prints, Posters, Calendars:
Carmen Leitner
E-mail: chem-reprints@wiley-vch.de
Fax: (+49) 6201–606-331
Telephone: (+49) 6201–606-327

Copyright Permission:
Bettina Loycke
E-mail: rights-and-licences@wiley-vch.de
Fax: (+49) 6201–606-332
Telephone: (+49) 6201–606-280

Online Open:
Margitta Schmitt, Carmen Leitner
E-mail: angewandte@wiley-vch.de
Fax: (+49) 6201–606-331
Telephone: (+49) 6201–606-315

Subscriptions:
www.wileycustomerhelp.com
Fax: (+49) 6201–606-184
Telephone: 0800 1800536 (Germany only)
+44(0) 1865476721 (all other countries)

Advertising:
Marion Schulz
E-mail: mschulz@wiley-vch.de
jspiess@wiley-vch.de
Fax: (+49) 6201–606-550
Telephone: (+49) 6201–606-565

Courier Services:
Boschstrasse 12, 69469 Weinheim

Regular Mail:
Postfach 101161, 69451 Weinheim

Angewandte Chemie International Edition is a journal of the Gesellschaft Deutscher Chemiker (GDCh), the largest chemistry-related scientific society in continental Europe. Information on the various activities and services of the GDCh, for example, cheaper subscription to *Angewandte Chemie International Edition*, as well as applications for membership can be found at **www.gdch.de** or can be requested from GDCh, Postfach 900440, D-60444 Frankfurt am Main, Germany.

GDCh
GESELLSCHAFT
DEUTSCHER CHEMIKER

Service

Author Profile

*“My favorite author is Lao Tzu.
What I look for first in a publication is the ‘flash’ that makes me think ‘a-ha’ …”*
This and more about Chao-Jun Li can be found on page 1082.

News


M. D. Burke


V. M. Dong


B. List


A. J. Phillips


K. Johnsson


M. S. P. Sansom


J.-P. Sauvage


H.-J. Freund


S. Röhrig

Books

Discovering Chemistry with Natural Bond Orbitals — Frank Weinhold, Clark E. Landis — *reviewed by J. Harvey* ____ **1085**

Highlights

Photoelectrochemistry

M. Antonietti* ____ **1086 – 1087**

On the Way to Artificial Photosynthesis: Simple Materials and System Designs for Photoelectrodes

For commercial viability new technologies for the sustainable generation of energy should be simple and efficient. Photoelectrodes made of boron arsenide are the latest advance: they can be synthesized easily directly from the elements and convert sunlight into electric current.

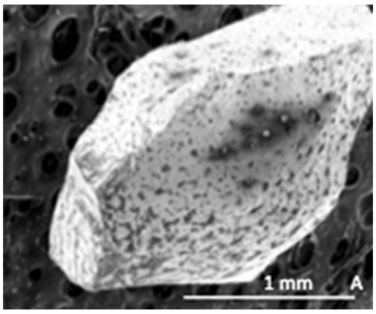

Essays

Microwave Chemistry

C. O. Kappe,* B. Pieber, D. Dallinger ____ **1088 – 1094**

Microwave Effects in Organic Synthesis: Myth or Reality?

It's not magic! The effects observed in microwave-irradiated chemical transformations can in most cases be rationalized by purely bulk thermal phenomena associated with rapid heating to elevated temperatures. As discussed in this Essay, the existence of so-called nonthermal or specific microwave effects is highly doubtful.

For the USA and Canada: ANGEWANDTE CHEMIE International Edition (ISSN 1433-7851) is published weekly by Wiley-VCH, PO Box 191161, 69451 Weinheim, Germany. Air freight and mailing in the USA by Publications Expediting Inc., 200 Meacham Ave., Elmont, NY 11003. Periodicals postage paid at Jamaica, NY 11431. US POSTMASTER: send address changes to *Angewandte Chemie*, Journal Customer Services, John Wiley & Sons Inc., 350 Main St., Malden, MA 02148-5020. Annual subscription price for institutions: US$ 11.738/10.206 (valid for print and electronic / print or electronic delivery); for individuals who are personal members of a national chemical society prices are available on request. Postage and handling charges included. All prices are subject to local VAT/ sales tax.

Minireviews

Nanostructures

Biomass is an abundant source of chemically diverse macromolecules. Much current effort is focused on the breakdown of these molecules into fuels or platform molecules. However, there is growing interest in using biopolymers directly to create nanostructured materials. It is highlighted how biopolymers are providing new directions in the synthesis of nanostructured materials.

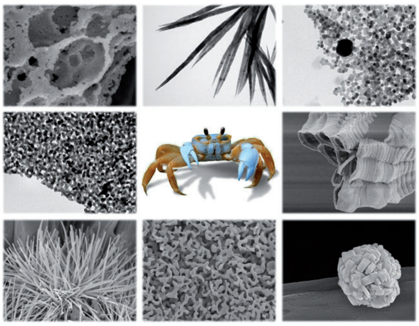

Reviews

Medicinal Chemistry

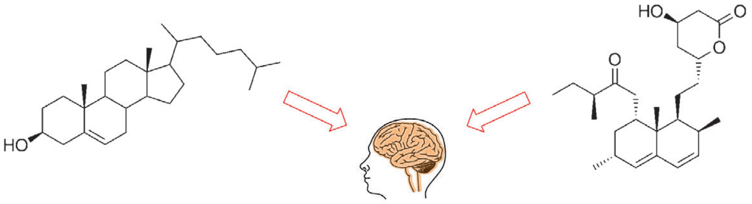

Cholesterol (left-hand structure) is an essential component of lipid rafts, in which the biosynthesis of neurotoxic β-amyloid occurs. By blocking the synthesis of cholesterol, statins (right-hand structure: lovastatin) are able to decrease the amyloid load in the central nervous system and lower the risk of dementia and Alzheimer’s disease. This behavior is strongly supported by the pleiotropic effects of statins on isoprenylation and neuroinflammation.

Communications

Hierarchically Ordered Structures

Frontispiece

A chemically patterned surface was formed by controlled evaporative self-assembly of concentric polymer stripes, followed by the removal of weakly deposited polymer, giving ultrathin polymer stripes with a width gradient on the Si substrate (see picture). A thin film of diblock copolymer hierarchically self-assembled on the ultrathin polymer stripes, giving arrays of nanocylinders perpendicular to the surface of the film.

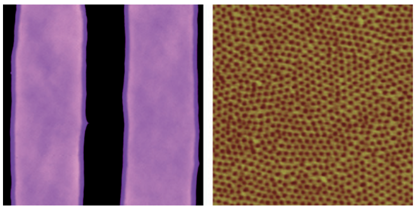

The German Chemical Society (GDCh) invites you to:

Angewandte Anniversary Symposium

125 JAHRE

Eine Zeitschrift der Gesellschaft Deutscher Chemiker

GDCh

Tuesday, March 12, 2013

Henry Ford Building / FU Berlin

Speakers


Carolyn R.
Bertozzi


François
Diederich


Alois
Fürstner


Roald Hoffmann
(Nobel Prize 1981)


Susumu
Kitagawa


Jean-Marie Lehn
(Nobel Prize 1987)


E.W. “Bert”
Meijer


Frank
Schirrmacher
(Publisher, *FAZ*)


Robert
Schlögl


George M.
Whitesides


Ahmed Zewail
(Nobel Prize 1999)

Freie Universität Berlin

Register now:

angewandte.org/symposium

WILEY-VCH

GDCh
GESELLSCHAFT
DEUTSCHER CHEMIKER

PSJ-12-50223_gu

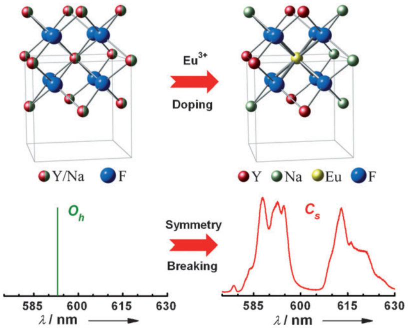

High-resolution photoluminescence spectroscopy employing Eu^{3+} as the structural probe unambiguously revealed a universal breakdown of crystallographic site symmetry in lanthanide-doped disordered crystals. The spectroscopic site symmetries of Eu^{3+} descend from crystallographic O_h to C_s (or C_2) in α-NaYF$_4$, and from crystallographic C_{3h} to C_s in β-NaYF$_4$, which were further verified by crystal-field level fitting.

Lanthanides

D. T. Tu, Y. S. Liu, H. M. Zhu, R. F. Li, L. Q. Liu, X. Y. Chen* ______ **1128 – 1133**

Breakdown of Crystallographic Site Symmetry in Lanthanide-Doped NaYF$_4$ Crystals

---

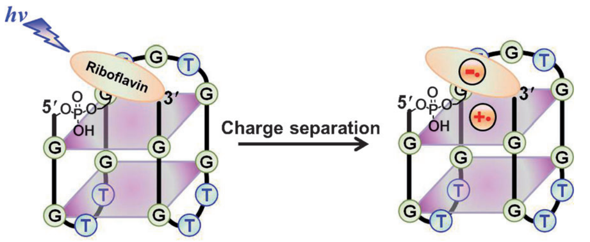

Hole trapping: The hole transfer and trapping in a G-quadruplex has been investigated using laser flash photolysis and pulse radiolysis. The results show that the charge separation in the G-quadruplex takes place efficiently between riboflavin and G-bases because of the excellent hole-trapping ability of planar G-quartets.

Photochemistry

J. Choi, J. Park, A. Tanaka, M. J. Park, Y. J. Jang, M. Fujitsuka, S. K. Kim,* T. Majima* ______ **1134 – 1138**

Hole Trapping of G-Quartets in a G-Quadruplex

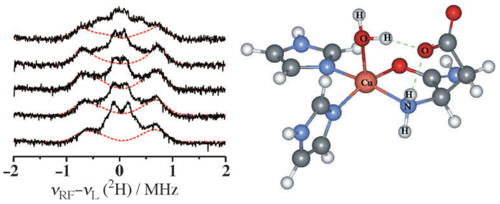

The copper(II) ion coordination mode of Cu^{II}-Aβ(1–16) at physiological pH was characterized by 34 GHz pulsed ENDOR spectroscopy. ^{1}H/^{2}H ENDOR and ^{14}N ENDOR demonstrate the NH$_2$ terminus of aspartic acid is an equatorial ligand of Cu^{II}, and ^{17}O ENDOR together with ^{1}H ENDOR suggest that water is an axial ligand (see picture; Cu pink, O red, N blue).

Copper Amyloid Peptide

D. Kim, N. H. Kim, S. H. Kim* ______ **1139 – 1142**

34 GHz Pulsed ENDOR Characterization of the Copper Coordination of an Amyloid β Peptide Relevant to Alzheimer's Disease

---

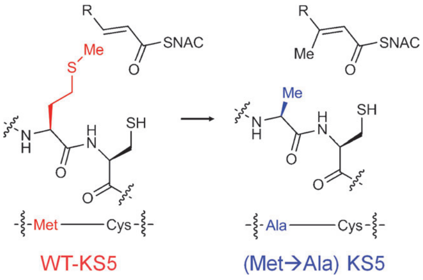

Branching out: The substrate specificity profiles for a range of ketosynthase (KS) domains from *trans*-AT PKSs are reported. Evidence is provided that a sterically demanding amino acid residue adjacent to the active-site Cys residue confers specificity towards non-β-methyl-branched substrates (see scheme).

Polyketide Biosynthesis

M. Jenner, S. Frank, A. Kampa, C. Kohlhaas, P. Pöplau, G. S. Briggs, J. Piel,* N. J. Oldham* ______ **1143 – 1147**

Substrate Specificity in Ketosynthase Domains from *trans*-AT Polyketide Synthases

Nanostructures

Y. Zhang, J. Qian, D. Wang, Y. Wang, S. He* ———— 1148 – 1151

Multifunctional Gold Nanorods with Ultrahigh Stability and Tunability for In Vivo Fluorescence Imaging, SERS Detection, and Photodynamic Therapy

Multimodal: Gold nanorods are coated with silica/polymer mutilayers, doped with surface-enhance Raman scattering (SERS) and fluorescence agents as well as photosensitizers. The structural and optical properties are tunable and stable in solutions and in living bodies. A real-time and specific in vivo SERS and fluorescence detection method using this structure is applied for tumor detection and subsequent photodynamic therapy (PDT).

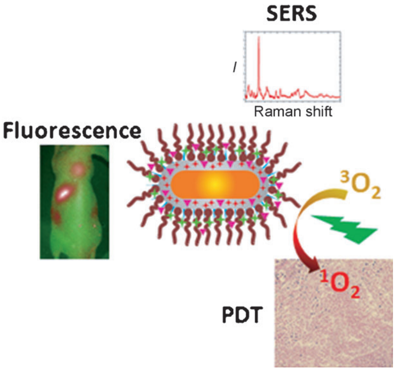

Nanoparticles

E. C. Cho, Y. Zhang, X. Cai, C. M. Moran, L. V. Wang,* Y. Xia* ———— 1152 – 1155

Quantitative Analysis of the Fate of Gold Nanocages In Vitro and In Vivo after Uptake by U87-MG Tumor Cells

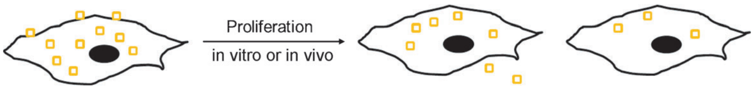

Not always equal: When a mother cell that contains Au nanocages divides, the nanoparticles are unequally distributed between the two daughter cells. This unequal distribution of nanoparticles as well as their clearance from the cells (see picture) is quantitatively analyzed both in vitro and in vivo using two-photon microscopy and photoacoustic microscopy, respectively.

Nanocomposite Hydrogels

N. S. Kehr,* E. A. Prasetyanto, K. Benson, B. Ergün, A. Galstyan, H.-J. Galla ———— 1156 – 1160

Periodic Mesoporous Organosilica-Based Nanocomposite Hydrogels as Three-Dimensional Scaffolds

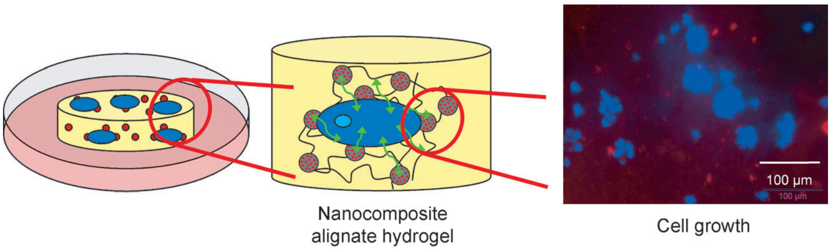

Dye-loaded periodic mesoporous organosilica particles functionalized with bioactive molecules were used for the generation of a nanocomposite alginate hydrogel. The affinity of cells was up to four times higher with the embedded particles than with simple alginate hydrogel, caused by both the nanometer-scale particle itself and its bioactive functionalization.

Imaging Agents

S. Geninatti Crich,* D. Alberti, I. Szabo, S. Aime, K. Djanashvili* ———— 1161 – 1164

MRI Visualization of Melanoma Cells by Targeting Overexpressed Sialic Acid with a Gd^{III}-dota-en-pba Imaging Reporter

Front Cover

By design: The novel MRI reporter Gd^{III}-dota-en-pba (see picture) selectively binds to sialic acid residues, which are overexpressed on tumors. This imaging reporter accumulates in a murine melanoma B16-F10 mice xenograft and from the MRI signal intensity it is possible to quantify the sialic acid concentration that is directly associated with tumor malignancy.

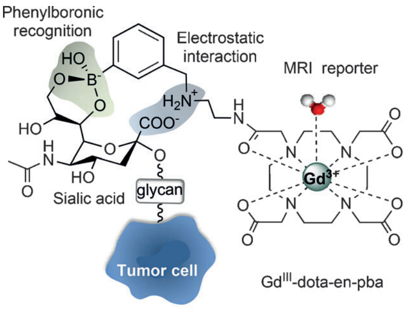

Nanocrystal Sensors

E. R. Kay, J. Lee, D. G. Nocera,
M. G. Bawendi* ________ 1165 – 1169

Conformational Control of Energy Transfer: A Mechanism for Biocompatible Nanocrystal-Based Sensors

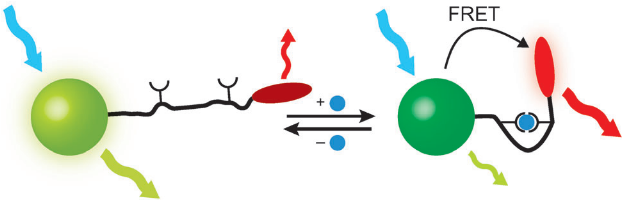

Know when to fold ’em: Combination of a pH-triggered oligonucleotide conformational switch with fluorescent nanocrystals gives a sensitive pH nanosensor (see scheme). Analyte-dependent conformational changes control the distance between the nanocrystal energy donor (green) and a FRET acceptor (red), which results in a reporter for pH values in individual endosomes of living cells.

X-ray Spectroscopy

M. M. van Schooneveld,* R. W. Gosselink,
T. M. Eggenhuisen, M. Al Samarai,
C. Monney, K. J. Zhou, T. Schmitt,
F. M. F. de Groot* ________ 1170 – 1174

A Multispectroscopic Study of 3 d Orbitals in Cobalt Carboxylates: The High Sensitivity of 2p3d Resonant X-ray Emission Spectroscopy to the Ligand Field

d–d excitations in detail: High-resolution 2p3d resonant X-ray emission spectroscopy (RXES) allows the observation of more as well as more intense d–d excitations than UV/Vis spectroscopy does as demonstrated on cobalt(II) carboxylates. Together with ligand field multiplet (LFM) calculations this allows their detailed electronic structure description, while 2p X-ray absorption spectroscopy (XAS) cannot discriminate these transition metal compounds.

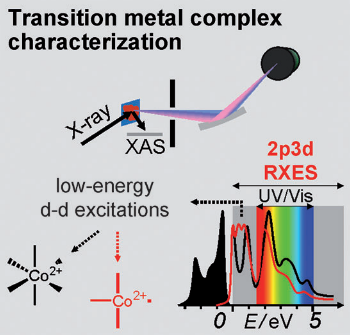

Back Cover

Bioluminescence

R. Kojima, H. Takakura, T. Ozawa, Y. Tada,
T. Nagano,* Y. Urano* ____ 1175 – 1179

Rational Design and Development of Near-Infrared-Emitting Firefly Luciferins Available In Vivo

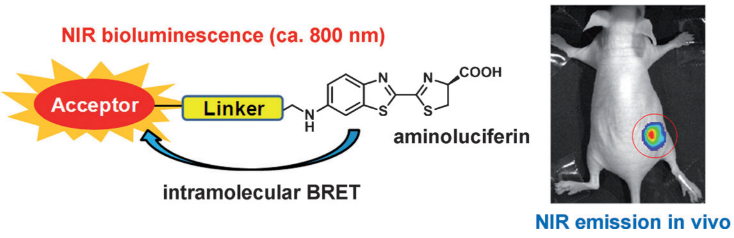

Shine on: A new rational design strategy for near-infrared-emitting firefly luciferins that are available in vivo has been developed using intramolecular bioluminescence resonance energy transfer (BRET). The emission wavelength could be freely tuned by the choice of BRET acceptor, and NIR bioluminescence could be detected in living cells and mice without the need for luciferase manipulation.

Color Modulation

T. Bhuvana, B. Kim, X. Yang, H. Shin,
E. Kim* ____________ 1180 – 1184

Reversible Full-Color Generation with Patterned Yellow Electrochromic Polymers

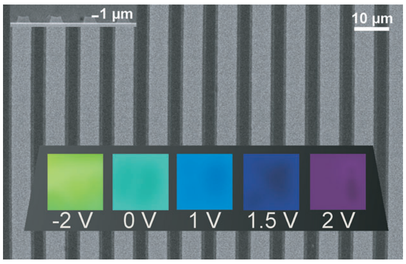

A different light: The yellow electrochromic copolymer, propylenedioxythiophene phenylene P(ProDOT-Ph) is patterned by the micromolding in capillaries (MIMIC) process to fabricate line gratings. Under illumination by white light, colors are generated by diffraction and can be changed by applying an external voltage (see picture). The diffracted color is blue shifted by electrochemical doping, a process that is completely reversible.

Spin Crossover

T. Q. Hung, F. Terki,* S. Kamara,
M. Dehbaoui, S. Charar, B. Sinha,
C. G. Kim,* P. Gandit, I. A. Gural'skiy,
G. Molnar, L. Salmon, H. J. Shepherd,
A. Bousseksou* ______ **1185 – 1188**

Room Temperature Magnetic Detection of Spin Switching in Nanosized Spin-Crossover Materials

Inside Cover

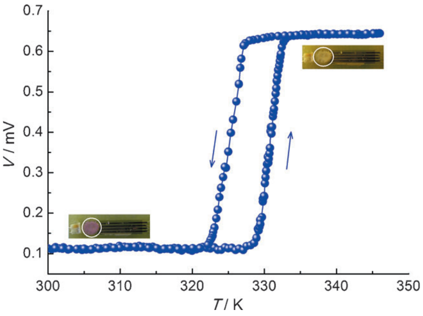

Building a better SQUID: A prototype for a SQUID-like magnetometry device for the indirect detection of room-temperature switching in spin-crossover nanoparticles has been developed and used in the study of $[Fe(hptrz)_3](OTs)_2$ (hptrz = 4-heptyl-1,2,4-triazole, OTs = *p*-toluenesulfonyl) nanoparticles, as a proof of concept for this novel micromagnetometry approach. The method provides significant benefits over conventional SQUID and nano-SQUID techniques.

DNA Nanotechnology

A. J. Genot, J. Bath,
A. J. Turberfield* ______ **1189 – 1192**

Combinatorial Displacement of DNA Strands: Application to Matrix Multiplication and Weighted Sums

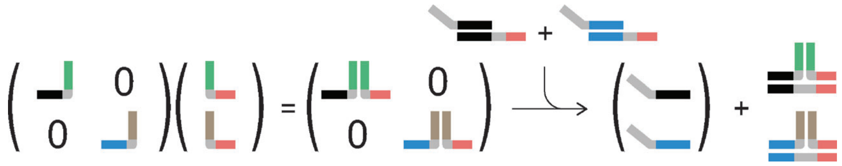

DNA multiplication tables: A combinatorial mechanism for DNA strand displacement shares the same structure as matrix multiplication (see scheme). This system can be used to perform linear operations on DNA concentrations, such as the calculation of a weighted sum.

DNA Nanotechnology

S. H. Ko, K. Du, J. A. Liddle* **1193 – 1197**

Quantum-Dot Fluorescence Lifetime Engineering with DNA Origami Constructs

Inside Back Cover

Single-molecule GPS: The average photon count rate and lifetime of a quantum dot (Qdot) have been controlled by varying the geometrical configuration of Qdot–gold nanoparticle (AuNP) conjugates on DNA origami. With a 3D real-time single-molecule tracking system, which allows the DNA templates to be kept in their native state in solution, the influence of AuNPs on the Qdot lifetime is determined (see picture).

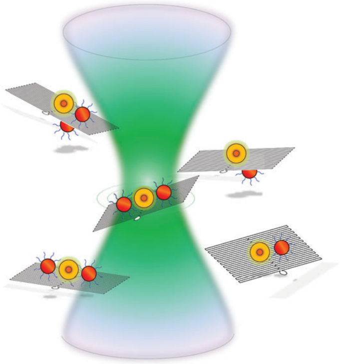

Spin Crossover

X. Bao, H. J. Shepherd, L. Salmon,
G. Molnár, M.-L. Tong,*
A. Bousseksou* ______ **1198 – 1202**

The Effect of an Active Guest on the Spin Crossover Phenomenon

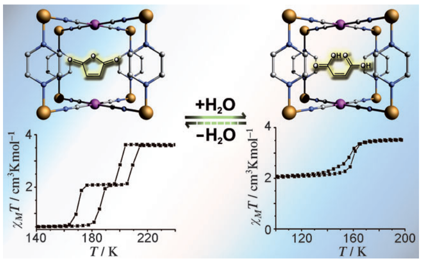

Throw the switch: A new strategy for regulating spin crossover (SCO) properties by the control of an active guest molecule is proposed. As a proof of concept, maleic anhydride was incorporated into a microporous {Fe(pyrazine)$[Pt(CN)_4]$} framework material and chemically switched to maleic acid, thus modifying the SCO properties (see picture).

Post-Translational Modification

Q. Zhou, M. Hu, W. Zhang, L. Jiang,
S. Perrett, J. Z. Zhou,
J. Y. Wang* ________ 1203 – 1207

Probing the Function of the Tyr-Cys Cross-Link in Metalloenzymes by the Genetic Incorporation of 3-Methylthiotyrosine

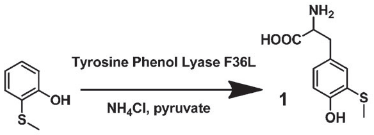

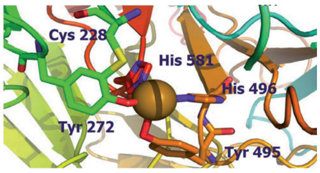

Efficient multiple-electron redox reactions are performed by galactose oxidase, cysteine dioxygenase, sulfite reductase, and cytochrome c nitrite reductase. A post-translationally modified tyrosine–cysteine cross-link (Tyr-Cys) in their active sites is essential for their functions.

Analytical Methods

S. Kubo, N. Nishida, Y. Udagawa,
O. Takarada, S. Ogino,
I. Shimada* ________ 1208 – 1211

A Gel-Encapsulated Bioreactor System for NMR Studies of Protein–Protein Interactions in Living Mammalian Cells

Staying alive: The major limitation of in-cell NMR spectroscopy methods is the occurrence of cell death during the NMR measurement. To overcome this problem, a bioreactor was utilized that can perfuse the cells in the NMR tube, thereby maintaining the conditions for more than 5 h. By using the bioreactor, the binding site of an externally introduced protein for an endogenous molecule in HeLa S3 cells was identified.

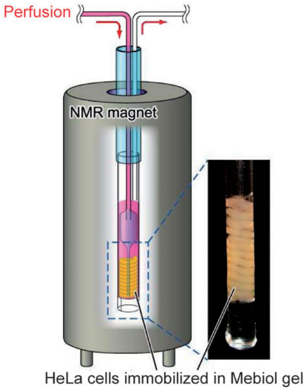

DNA Structures

J.-L. H. A. Duprey, Y. Takezawa,
M. Shionoya* ________ 1212 – 1216

Metal-Locked DNA Three-Way Junction

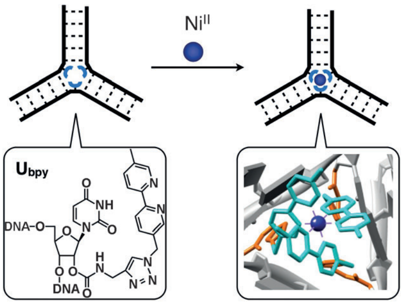

Three-way split: A postsynthetic click reaction has resulted in the conjugation of three bipyridine ligands at the core of a DNA three-way junction structure (see picture). Melting curve analyses revealed that Ni^{II} ions significantly stabilize the junction structure through the formation of a $[Ni(bpy)_3]^{2+}$ complex which cross-links three strands. The metal complex shows a diastereomeric preference, thus indicating a chirality transfer from the DNA.

Plasmon-Enhanced Fluorescence

H. Yuan, S. Khatua, P. Zijlstra,
M. Yorulmaz, M. Orrit* ________ 1217 – 1221

Thousand-fold Enhancement of Single-Molecule Fluorescence Near a Single Gold Nanorod

Single molecules: Large enhancements of single-molecule fluorescence up to 1100 times by using synthesized gold nanorods are reported (see picture). This high enhancement is achieved by selecting a dye with its adsorption and emission close to the surface plasmon resonance of the gold nanorods.

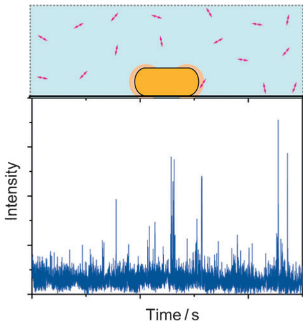

NMR Spectroscopy

A. Zagdoun, A. J. Rossini, M. P. Conley, W. R. Grüning, M. Schwarzwälder, M. Lelli, W. T. Franks, H. Oschkinat, C. Copéret, L. Emsley,* A. Lesage* ____ 1222–1225

Improved Dynamic Nuclear Polarization Surface-Enhanced NMR Spectroscopy through Controlled Incorporation of Deuterated Functional Groups

In a spin: The use of deuterated surface passivation agents is shown to restore dynamic nuclear polarization (DNP) surface-enhanced NMR signals that are reduced in substrates containing methyl groups, while still protecting sensitive sites on the surface (see picture). Furthermore, apolar groups such as [D$_9$]-trimethylsiloxy (TMS) repel radicals (yellow) away from the surface, thus diminishing detrimental paramagnetic effects induced by radical proximity.

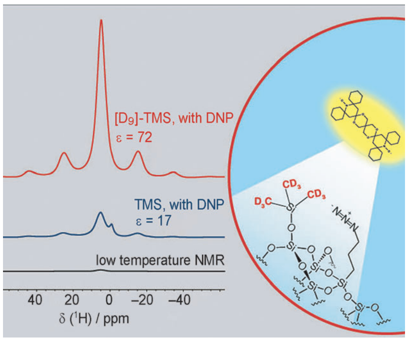

Gas-Phase Reactions

J.-B. Ma, Z.-C. Wang, M. Schlangen,* S.-G. He,* H. Schwarz* ____ 1226–1230

On the Origin of the Surprisingly Sluggish Redox Reaction of the N_2O/CO Couple Mediated by $[Y_2O_2]^{+\bullet}$ and $[YAlO_2]^{+\bullet}$ Cluster Ions in the Gas Phase

Kinetic energy barriers that have entirely different origins are the reasons for the impedance of the catalytic N_2O/CO redox cycle mediated by both $[YAlO_2]^{+\bullet}$ and $[Y_2O_2]^{+\bullet}$ clusters (see scheme). While oxidation with N_2O is the bottleneck for $[YAlO_2]^{+\bullet}$, oxidation of $[Y_2O_2]^{+\bullet}$ with N_2O is possible, but reduction of $[Y_2O_3]^{+\bullet}$ by CO is prevented. This arises because of "doping" effects which can control local charges and spin distributions.

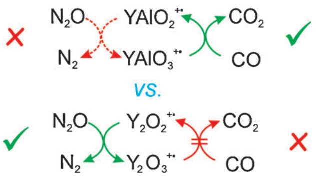

Antitubercular Prodrugs

Q. Wang, F. Song, X. Xiao, P. Huang, L. Li, A. Monte, W. M. Abdel-Mageed, J. Wang, H. Guo, W. He, F. Xie, H. Dai, M. Liu, C. Chen, H. Xu, M. Liu, A. M. Piggott, X. Liu,* R. J. Capon,* L. Zhang* ____ 1231–1234

Abyssomicins from the South China Sea Deep-Sea Sediment *Verrucosispora* sp.: Natural Thioether Michael Addition Adducts as Antitubercular Prodrugs

From the deep: The title actinomycete yielded three new abyssomicins J–L. The dimeric thioether J (see scheme) represents a unique example of a masked Michael acceptor with anti-TB properties. Mechanistic insights into the biosynthesis, biomimetic synthesis, stability, and biological mechanism of action of abyssomicins aid our understanding of, and prospects for the development of Michael-acceptor-based drugs.

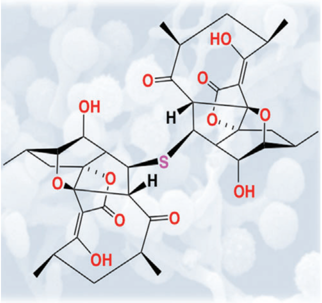

Nanoporous Materials

M. Hu,* S. Ishihara, Y. Yamauchi* ____ 1235–1239

Bottom-Up Synthesis of Monodispersed Single-Crystalline Cyano-Bridged Coordination Polymer Nanoflakes

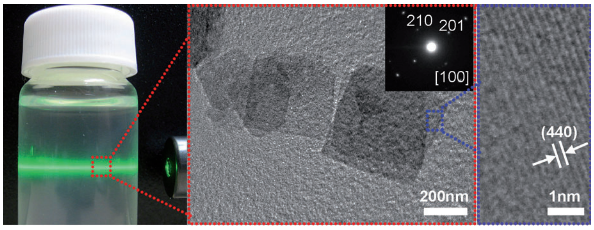

A two-dimensional morphology characterizes the nanoflakes that are obtained in the bottom-up synthesis of a single-crystalline coordination polymer, $Ni(H_2O)_2[Ni(CN)_4]\cdot xH_2O$. The 10 nm-thick nanoflakes are well-dispersed in solution and have a very high accessible surface area (240 m^{2}g^{-1}). Thermal treatment leads to nanoporous NiO with retention of the original flake morphology.

C–H Functionalization

P.-S. Lee, N. Yoshikai* ______ **1240 – 1244**

Aldimine-Directed Branched-Selective Hydroarylation of Styrenes

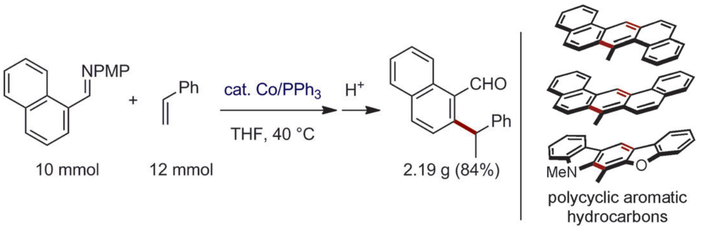

Branching out: A simple and inexpensive cobalt/triarylphosphine catalyst promotes aldimine-directed hydroarylation of styrene with high branched regioselectivity to afford 1,1-diarylethane derivatives in good yields under mild reaction conditions. The *ortho*-formyl group in the hydroarylation products is amenable to dehydrative cyclization, to give fused polycyclic aromatic hydrocarbons, as well as decarbonylative removal.

C–H Activation

G. Li, D. Leow, L. Wan,
J.-Q. Yu* ______ **1245 – 1247**

Ether-Directed *ortho*-C–H Olefination with a Palladium(II)/Monoprotected Amino Acid Catalyst

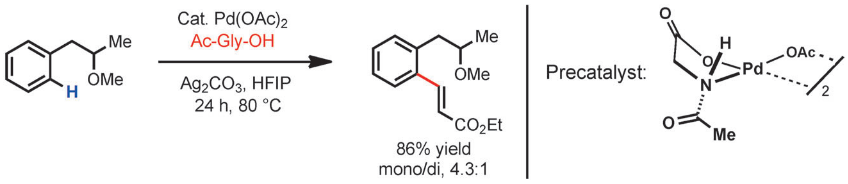

Weak coordination is powerful! A Pd^{II}-catalyzed olefination of *ortho*-C–H bonds of arenes directed by weakly coordinating ethers is developed by using monoprotected amino acid (MPAA) ligands. This finding provides a method for chemically modifying ethers, which are abundant in natural products and drug molecules. HFIP = hexafluoroisopropanol.

Photoanodes

Y. Hou, F. Zuo, A. Dagg,
P. Y. Feng* ______ **1248 – 1252**

A Three-Dimensional Branched Cobalt-Doped α-Fe_2O_3 Nanorod/$MgFe_2O_4$ Heterojunction Array as a Flexible Photoanode for Efficient Photoelectrochemical Water Oxidation

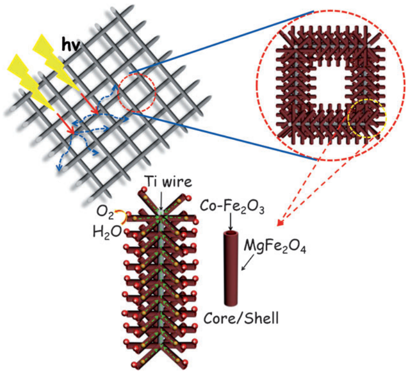

Hitting water with nanotrees: A three-dimensional branched heterojunction array for water oxidation based on cobalt-doped α-Fe_2O_3 nanorod cores and $MgFe_2O_4$ shells has been synthesized. Such an architecture not only has a large surface area and excellent light absorption properties, and shows fast charge transport, but also exhibits a very high photoelectrochemical activity for water oxidation and a high stability.

Composite Membranes

A. F. Bushell, P. M. Budd,* M. P. Attfield,
J. T. A. Jones, T. Hasell, A. I. Cooper,*
P. Bernardo, F. Bazzarelli, G. Clarizia,
J. C. Jansen* ______ **1253 – 1256**

Nanoporous Organic Polymer/Cage Composite Membranes

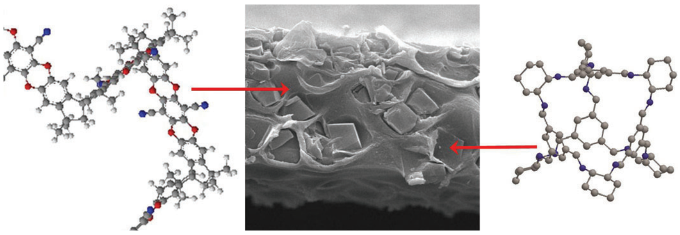

Organic–organic composite membranes are prepared by in situ crystallization of cage molecules in a polymer of intrinsic microporosity. This allows a direct one-step route to mixed-matrix membranes, starting with a homogeneous molecular solution. Extremely high gas permeabilities are achieved, even after ageing for more than a year, coupled with good selectivity for applications such as CO_2 recovery.

Asymmetric Catalysis

J. Fournier, O. Lozano, C. Menozzi,
S. Arseniyadis,* J. Cossy* **1257 – 1261**

Palladium-Catalyzed Asymmetric Allylic Alkylation of Cyclic Dienol Carbonates: Efficient Route to Enantioenriched γ-Butenolides Bearing an All-Carbon α-Quaternary Stereogenic Center

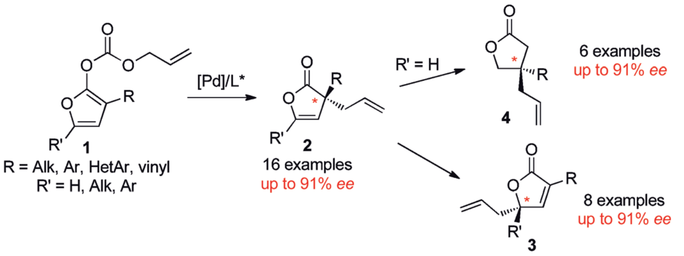

Alpha, beta, gamma: Allyl dienol carbonates (**1**) served as substrates for the title reaction to afford the furanones **2** in both high yields and high enantioselectivities. These furanones were eventually converted into valuable building blocks including γ-tertiary and γ-quaternary furanones (**3**) as well as β-quaternary butyrolactones (**4**). This method was used as a key step in the total synthesis of (−)-nephrosteranic acid and (−)-roccellaric acid.

Photodynamic Therapy

J. Wang, J. Newman, Jr., S. L. H. Higgins,
K. M. Brewer, B. S. J. Winkel,
K. J. Brewer* **1262 – 1265**

Red-Light-Induced Inhibition of DNA Replication and Amplification by PCR with an Os/Rh Supramolecule

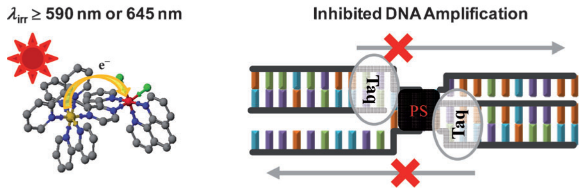

Bimetallic: Upon irradiation with light in the phototherapeutic window, the bimetallic complex $[(bpy)_2Os(dpp)RhCl_2(phen)]^{3+}$ binds to and cleaves DNA through an oxygen-independent mechanism. PCR is used as a model for in vitro DNA replication. The results show that the metal complex does not interfere with DNA amplification in the dark without O_2, but completely inhibits DNA amplification in samples exposed to red light. Taq = polymerase, PS = photosensitizer.

Heterocycles

F. Zhan, G. Liang* **1266 – 1269**

Formation of Enehydrazine Intermediates through Coupling of Phenylhydrazines with Vinyl Halides: Entry into the Fischer Indole Synthesis

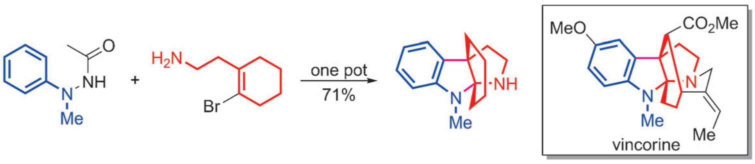

Cut to the chase: Direct formation of an enehydrazine, an intermediate in the classic Fischer indole synthesis, solves the regioselectivity problem associated with indolization. This approach not only achieves selective synthesis of indoles through proper selection of the vinyl halide, but also leads to quick construction of desoxyeseroline and esermethole, as well as the key structural motif in the *Akuammiline* alkaloid vincorine.

Biomass

E. I. Gürbüz, J. M. R. Gallo, D. M. Alonso,
S. G. Wettstein, W. Y. Lim,
J. A. Dumesic* **1270 – 1274**

Conversion of Hemicellulose into Furfural Using Solid Acid Catalysts in γ-Valerolactone

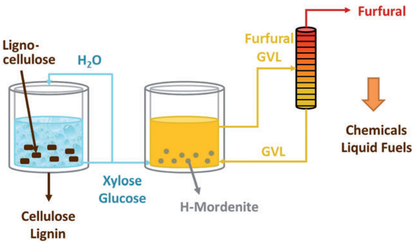

Hold the water: The hemicellulose fraction of lignocellulose can be converted into furfural in high yields (80%) using solid acid catalysts (H-mordenite) in a monophasic system with γ-valerolactone (GVL) as the solvent. Furfural degradation reactions are decreased significantly when the water concentration in GVL is minimized, thus resulting in high furfural yields.

Chiral Nanocrystals

A. Ben-Moshe, A. O. Govorov,
G. Markovich* 1275 – 1279

Enantioselective Synthesis of Intrinsically Chiral Mercury Sulfide Nanocrystals

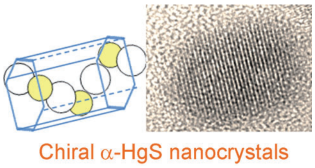

Equal and opposite: A chiral surfactant molecule was used to induce high enantioselectivity in the transformation from the achiral phase of mercury sulfide, probably through binding of the surfactant thiolate groups to Hg ions in the forming crystal. The generation of truly chiral inorganic nanocrystals of tailored size and shape should be useful for many applications, such as enantioselective catalysis and sensing.

Oxidation of Methane

M. H. Ab Rahim, M. M. Forde,
R. L. Jenkins, C. Hammond, Q. He,
N. Dimitratos, J. A. Lopez-Sanchez,
A. F. Carley, S. H. Taylor, D. J. Willock,
D. M. Murphy, C. J. Kiely,
G. J. Hutchings* 1280 – 1284

Oxidation of Methane to Methanol with Hydrogen Peroxide Using Supported Gold–Palladium Alloy Nanoparticles

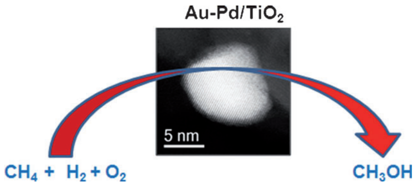

Direct and selective: Supported gold–palladium nanoparticles are active for the oxidation of methane, giving a high selectivity for the formation of methyl hydroperoxide and methanol, using hydrogen peroxide as the oxidant (see picture). The optimal methanol selectivity is achieved by performing the reaction in the presence of hydrogen peroxide that has been generated in situ from hydrogen and oxygen.

Iron catalysis

R. B. Bedford,* E. Carter, P. M. Cogswell,
N. J. Gower, M. F. Haddow, J. N. Harvey,
D. M. Murphy, E. C. Neeve,
J. Nunn 1285 – 1288

Simplifying Iron–Phosphine Catalysts for Cross-Coupling Reactions

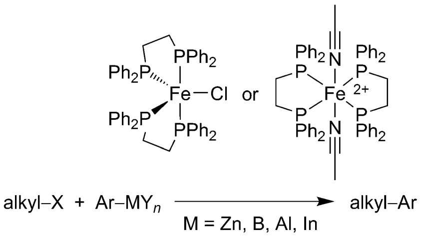

Any old iron? Iron catalysts based on the widely available diphosphine ligand bis(diphenylphosphino)ethane have not previously fared particularly well in iron-catalyzed cross-coupling processes. However, this turns out not to be due to any inherently poor performance associated with the ligand, but rather the need to form a bis-chelate complex, either before or during the formation of an active Fe^{I} species.

Buckybowls

T.-C. Wu, M.-K. Chen, Y.-W. Lee,
M.-Y. Kuo,* Y.-T. Wu* 1289 – 1293

Bowl-Shaped Fragments of C_{70} or Higher Fullerenes: Synthesis, Structural Analysis, and Inversion Dynamics

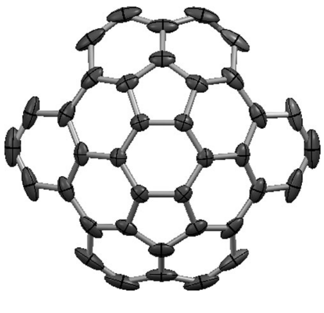

Super bowl: Fragments of C_{70} or higher fullerenes were easily prepared from 1,8-bis(arylethynyl)naphthalenes. The curved structures were identified by X-ray crystallography. These rigid bowl-shaped molecules have a deep bowl depth (approximately 2.30 Å) and their bowl inversions proceed via an S-shaped transition structure with a very high inversion barrier (approximately 80 kcal mol^{-1}).

Bioinorganic Chemistry

K. Park, T. Tsugawa, H. Furutachi, Y. Kwak, L. V. Liu, S. D. Wong, Y. Yoda, Y. Kobayashi, M. Saito, M. Kurokuzu, M. Seto, M. Suzuki,* E. I. Solomon* ______ 1294 – 1298

Nuclear Resonance Vibrational Spectroscopy and DFT study of Peroxo-Bridged Biferric Complexes: Structural Insight into Peroxo Intermediates of Binuclear Non-heme Iron Enzymes

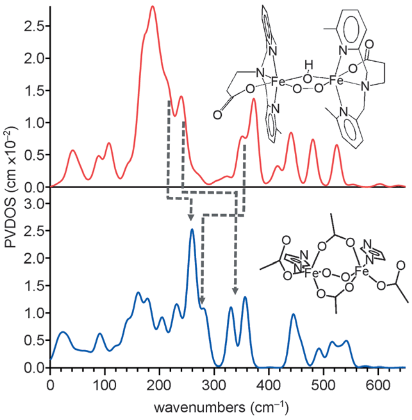

Low-frequency vibrational modes of peroxo-bridged high-spin biferric complexes have been observed using nuclear resonance vibrational spectroscopy (NRVS; see picture, PVDOS = partial vibrational density-of-states) and assigned using DFT calculations. Correlations between the spectral features and the structure of peroxo-bridged cores form a basis for structural elucidation of enzyme–peroxo intermediates.

Synthetic Methods

Y. Shang, X. Jie, J. Zhou, P. Hu, S. Huang, W. Su* ______ 1299 – 1303

Pd-Catalyzed C–H Olefination of (Hetero)Arenes by Using Saturated Ketones as an Olefin Source

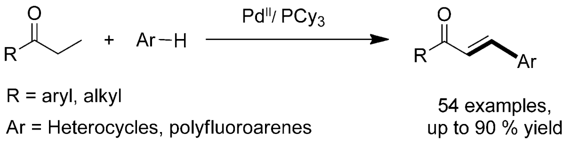

Tolerant: By using Pd(OAc)$_2$/PCy$_3$ as a catalyst, both electron-rich aromatic heterocycles and electron-deficient fluorobenzenes undergo the dehydrogenative cross-coupling with (hetero)aryl ethyl ketones in good yields. A broad range of functional groups is tolerated, thus providing a general method for the facile syntheses of chalcones or heterocyclic chalcone analogues. Furthermore, dialkyl ketones can also participate in this transformation.

Biosynthesis

VIP

Y. Li, E. Luxenburger, R. Müller* ______ 1304 – 1308

An Alternative Isovaleryl CoA Biosynthetic Pathway Involving a Previously Unknown 3-Methylglutaconyl CoA Decarboxylase

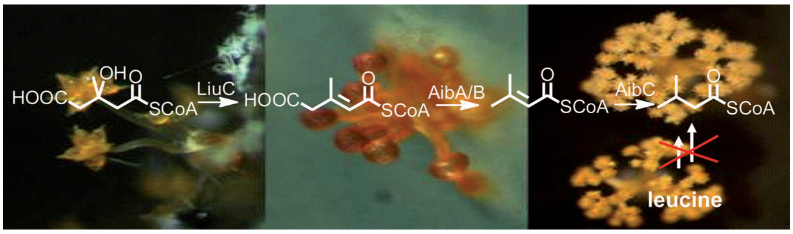

Take a detour: An alternative pathway to synthesize isovaleryl coenzyme A (CoA) has recently been suggested in myxobacteria, which is highly active when leucine is limited. Each enzymatic step of this unprecedented route has now been characterized and a novel 3-methylglutaconyl CoA decarboxylase identified that has apparently evolved from CoA transferases.

Protein Synthesis

F. Wintermann,* S. Engelbrecht* ______ 1309 – 1313

Reconstitution of the Catalytic Core of F-ATPase (αβ)$_3$γ from *Escherichia coli* Using Chemically Synthesized Subunit γ

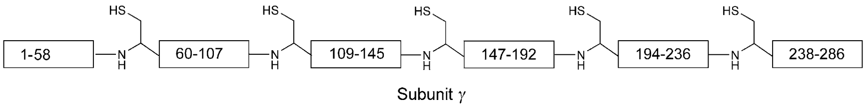

Hooking up: Subunit γ of an F-ATPase with 11 point mutations was ligated chemically from six peptides and then reconstituted with further subunits of the (αβ)$_3$γ catalytic core complex. The biologically active protein with 286 residues currently represents the longest nonredundant polypeptide chain synthesized by chemical means. The yields of the five consecutive ligations, especially the last three, dropped the total yield to only 0.005 %.

Transition-Metal Hydrides

M. Plois, W. Hujo, S. Grimme,
C. Schwickert, E. Bill, B. de Bruin,
R. Pöttgen, R. Wolf* ——— **1314 – 1318**

Open-Shell First-Row Transition-Metal Polyhydride Complexes Based on the *fac*-$[RuH_3(PR_3)_3]^-$ Building Block

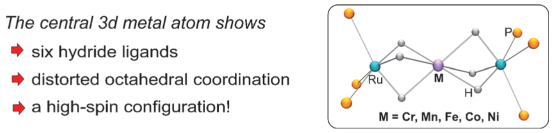

High-spin hydrides: A new class of stable paramagnetic polyhydride complexes $[M\{Ru(\mu\text{-}H)_3(PTol_3)_3\}_2]$ (M = Cr–Ni) with an unprecedented trinuclear arrangement has been synthesized. The high-spin central 3d metal ion is sandwiched between six hydride ligands in a distorted octahedral fashion.

Photoswitching

M. Han, R. Michel, B. He, Y.-S. Chen,
D. Stalke, M. John,
G. H. Clever* ——— **1319 – 1323**

Light-Triggered Guest Uptake and Release by a Photochromic Coordination Cage

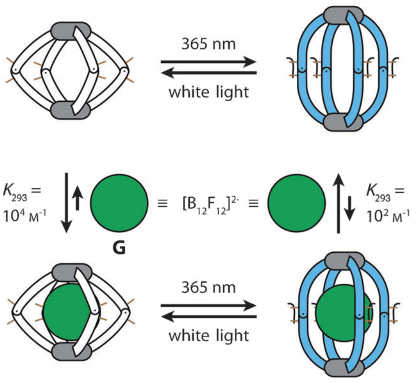

A guiding light is sufficient to switch back and forth between the flexible and the stretched, rigid form of a self-assembled coordination cage based on two square-planar-coordinated Pd^{II} ions and four ligands with a photochromic dithienylethene (DTE) backbone. The light-driven interconversion is clean and reversible and allows to control the encapsulation and release of the guest $[B_{12}F_{12}]^{2-}$.

Hypervalent Iodine Reagents

J. A. Souto, C. Martínez, I. Velilla,
K. Muñiz* ——— **1324 – 1328**

Defined Hypervalent Iodine(III) Reagents Incorporating Transferable Nitrogen Groups: Nucleophilic Amination through Electrophilic Activation

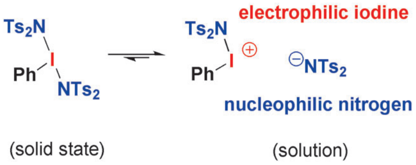

Only I and N: Hypervalent iodine(III) reagents with two reactive I–N single bonds have been isolated for the first time. Their solid-state and solution structures provide evidence for enhanced electrophilicity at iodine and nucleophilic character of the imine. As a result, improved reactivity in amination reactions and unprecedented nitrogen-transfer reactions under metal-free conditions are realized.

Gold Catalysis

A. S. K. Hashmi,* W. Yang, Y. Yu,
M. M. Hansmann, M. Rudolph,
F. Rominger ______________ **1329 – 1332**

Gold-Catalyzed Formal 1,6-Acyloxy Migration Leading to 3,4-Disubstituted Pyrrolidin-2-ones

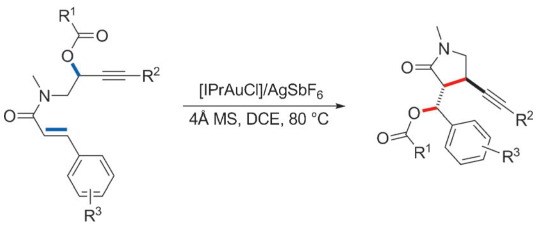

Mobile: The title reaction affords diastereomerically pure 3,4-disubstituted pyrrolidin-2-ones, which are important structural motifs in natural products, in good to high yields. Mechanistic investigations suggest the transformation proceeds through a tandem 1,3-acyloxy migration and a subsequent 1,5-acyloxy migration. DCE = 1,2-dichloroethane, IPr = 1,3-bis(2,6-diisopropylphenyl)imidazol-2-ylidene.

Supporting information is available on www.angewandte.org (see article for access details).

A video clip is available as Supporting Information on www.angewandte.org (see article for access details).

This article is available online free of charge (Open Access).

This article is accompanied by a cover picture (front or back cover, and inside or outside).

Check out these journals:

www.chemasianj.org

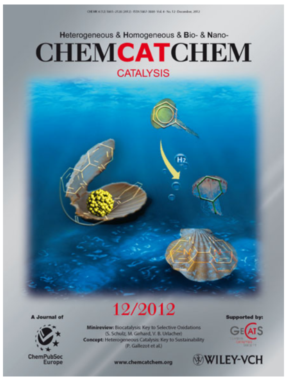

www.chemcatchem.org

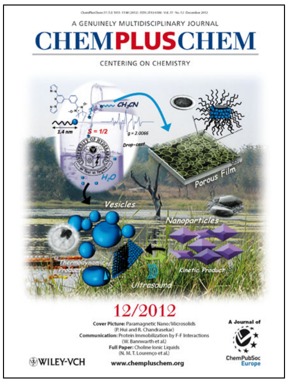

www.chempluschem.org

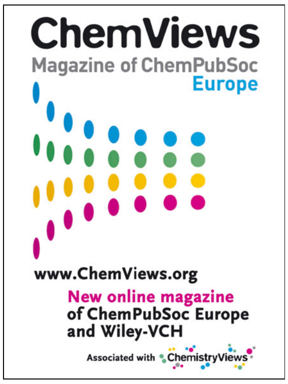

www.chemviews.org